Chapter 30
Safety Monitoring of Materials and Components of Nuclear Power Plants

A. Gokhman and F. Bergner

Abstract Cluster dynamics (CD) is used to study the evolution of the size distributions of vacancy clusters (VC), self-interstitial atom (SIA) clusters (SIAC) and Cr precipitates in neutron irradiated Fe-9at.%Cr and Fe-12.5at.%Cr alloys at $T = 573$ K with irradiation doses up to 1.5 dpa and a flux of 140 ndpa/s. Transmission electron microscopy (TEM) and small angle neutron scattering (SANS) data on the defect structure of this material irradiated at doses of 0.6 and 1.5 dpa are used to calibrate the model. For both alloys a saturation behavior has been found by CD for the free vacancy and free SIA concentrations as well as for the number density of the SIAC for the doses above 0.006 dpa. The CD simulations also indicate the presence of VC with radii less than 0.5 nm and a strong SIAC peak with a mean diameter of about 0.5 nm, both invisible in SANS and TEM experiments. CD modeling of Cr precipitates has been made taking into account the deviation of this system from the ideal cluster gas. A specific surface tension of about 0.17 J/m^2 between the α matrix and the Cr-rich α' precipitate and the rate at which *Cr* monomers are absorbed about 7.94 m^{-1} have been found as best fit values for reproducing the long-term Cr evolution in the irradiated Fe-12.5%Cr alloys observed by SANS. The change of the composition of Fe-Cr precipitates due to irradiation has been found.

Keywords Cluster dynamics • Neutron irradiation • Fe-Cr precipitates • Defect structure

A. Gokhman (✉)
South Ukrainian National Pedagogical University, 26 Staroportofrankovskaya, Odessa, Ukraine
e-mail: gokhman@paco.net

F. Bergner
Helmgoltz Center Dresden Rossendorf, Dresden, Germany

Y.N. Shunin and A.E. Kiv (eds.), *Nanodevices and Nanomaterials for Ecological Security*, NATO Science for Peace and Security Series B: Physics and Biophysics, DOI 10.1007/978-94-007-4119-5_30,

30.1 Introduction

Evaluation models for the process and accident analysis are being developed and validated to provide the safety monitoring of materials and components of nuclear power plants. The pressure vessel of a nuclear reactor (RPV) is of utmost importance for safety. The RPV steels are subject to operational loads, including those resulting from the radiation field generated by nuclear fission. Neutron irradiation leads to detrimental changes in macroscopic mechanical properties i.e. to the increase in yield strength and the reduction in fracture toughness. There are intense worldwide efforts to detect irradiation damage early to understand the underlying phenomena, to develop appropriate numerical models and to evaluate the implications for the RPV integrity. The present work has been extended to structural candidate materials for reactors of the 4th generation. The main focus is on the elucidation of the formation mechanisms of radiation defects on the nanometer scale. For that purpose the CD has been developed, which is validated by using SANS and TEM. Ferritic-martensitic chromium steels are candidate structural materials for the future generation nuclear reactors such as fusion or advanced high temperature reactors (Gen IV) or spallation sources because of their remarkable resistance to swelling and of their adequate mechanical properties. The investigation of neutron-irradiated binary Fe-Cr alloys by TEM [1] and SANS data [2–4] will significantly contribute to the understanding of the behavior of more complex alloys. For the purpose of predicting irradiation hardening it is necessary to know in detail the size distributions of vacancy clusters (VC), self-interstitial atom clusters (SIAC) and Cr precipitates formed under irradiation at any neutron dose. The latter can be obtained by means of CD. Solubility limit of Cr in Fe-Cr system is about 8.8at.% at $T = 573$ K[2]. Hence, deviation of the Cr precipitates ensemble from the ideal cluster gas [5] has been taken into account in CD modeling of Fe-9at.%Cr alloy and Fe-12.5at.%Cr alloy.

30.2 Irradiation Conditions and Experimental Data

The irradiation conditions and experimental results [1–4] are summarized below for the purpose of comparison with the CD simulations performed in this study. Both the industrial purity Fe-9at.%Cr alloy and Fe-12.5at.%Cr alloy (average grain size 1 μm, pre-existing dislocation density 5.5×10^{13} m^{-2}) were neutron-irradiated in the Callisto rig (IPS2) in the Belgian reactor (BR2). The irradiation temperature T of 573 K and the neutron flux of about 9×10^{17} n/m^{2}s ($E > 1$ MeV) were maintained. This flux corresponds to the dose rate of about 140 ndpa/s. The neutron exposure covered the range from 0.6 to 1.5 dpa.

TEM investigations of the Fe-12.5at.%Cr alloy [1] reveal the presence of dislocation loops of size 6 nm (in diameter) and a total loop density of about 1.73×10^{21} m^{-3} for both irradiation conditions, 0.6 and 1.5 dpa. No voids were

observed by TEM under these irradiation conditions. Irradiation-induced features with diameter of about 2 nm and volume fraction of (4.3 ± 0.4) % for both irradiation conditions and *A*-ratios (ratio of total and nuclear SANS intensity) of 2.07 ± 0.05 and 2.05 ± 0.05 for the dose of 0.6 and 1.5 dpa, respectively, have been found by SANS. These features were related to pure Cr precipitates in α-Fe as well as to α′ particles dispersed in the α-Fe matrix. A decrease [2] in the scattering cross-section of SANS with the decreasing scattering vector, *Q*, has been found as typical for the interference effects in concentrated alloys. According to the approach [6], the interference factor *S*(*Q*) has been determined for this *Q*-range [7]. Then, the mono-disperse hard-sphere model [8], taking into account the correlation between all hard spheres (depletion zones), has been applied to interpret the obtained interference factor. The volume fraction of the hard spheres has been found at 14.4% and 13.3% and the average distance between them at 2.38 and 1.97 nm for the irradiation doses of 0.6 and 1.5 dpa, respectively. The size distribution of the α′ particles[2] has been obtained by the indirect transformation method applied to the fitted measured nuclear scattering cross sections. The range of the *Q*-values has been restricted to the values greater than 1 nm^{-1} in the fit, where interference effect can be excluded.

According to TEM study [1], the population of dislocation loops decorated by Cr atoms with the diameter of about 7 and 13 nm and a total loop density of about 1.9×10^{21} m^{-3} and 1.7×10^{21} m^{-3} in the Fe-9at.%Cr alloy are formed due to irradiation with the dose of 0.6 and 1.5 dpa, respectively. SANS experiments [3] for both irradiation conditions indicate the two populations of irradiation-induced features with the radius, *R*, in the ranges, $R < 2.4$ nm and 2.4 nm $< R < 7$ nm, respectively. The A-ratio of these features is higher than of those expected for nanovoids and α′- particles, but smaller than of those expected for well-developed Cr-carbides. According to SANS the total volume fraction of irradiation-induced features slightly increases with neutron influence.

30.3 CD Master Equation

Defect structure of neutron irradiated Fe-Cr alloys consists of free vacancies, SIA, vacancy clusters, pure dislocation loops, dislocation loops decorated by Cr atoms and vacancy – Cr complexes as well as Cr precipitates and depends on the irradiation regime [9]. The CD model used in our study is close to the CD-P-VIC model [10], where the CD simulations are first performed for the free vacancies, SIA and point defect clusters and then, for the precipitates, taking into account the actual time dependence of the free point defect concentrations obtained in the first step. In addition [10], we take into account the Cr-effect on the SIA diffusivity according to the DFT calculations [11].

The assumptions used to study the evolution of the Cr precipitates need special attention. Two different mechanisms [9] have been suggested for the irradiation induced or enhanced formation of α′ precipitates in Fe-Cr alloys. The first mechanism suggested for the migration of Cr to the voids is the exchange of chromium

atoms with vacancies. This statement is in line with DFT calculations that predict a relatively low barrier for chromium atom exchange with a vacancy in iron [12]. The second proposed mechanism relies on the strong interaction between chromium atoms and SIA, leading to the transport of Cr atoms to SIA loops. According to TEM data [1], the first and the second mechanisms are observed in the irradiated Fe-12.5at.%Cr alloy and Fe-9at.%Cr alloy, respectively.

Another important thing here to be taken into account is the overlapping diffusion field effect and the frustrations effect in the considered materials that are typical for concentrated alloys [13–15]. Correction of the attachment coefficient of Cr to Cr precipitates is needed because a relatively high chromium concentration will be used in our study according to the method discussed in [13]. The frustration effect [14, 15] will be taken into account empirically by the use of the thermodynamic free energy expression from CALPHAD [16] with the correction suggested by Bonny et al. [17].

30.3.1 Matrix Defect System

The public domain library solver LSODA [18] has been used to integrate directly the master equation [19] for the study of the matrix defect subsystem containing free vacancies, spherical VC with sizes up to 1,000 vacancies, free SIA and planar SIAC with sizes up to 4,000 SIA. The attachment coefficients for the master equation [19] are determined in the diffusion limited regime and following the approach [20] for spherical VC and planar SIAC, respectively. The emission coefficients [19] are fixed using the detailed balance principle for both VC and SIAC. The values for the pre-existing dislocation density, ρ_0, and the average grain size, d, are taken from the experiment [1]. Other material parameters are found by fitting the results of the CD simulation to the condition of the best reproduction of the experimental data [1]. The only substantial change in the material parameters [19] is the SIA diffusivity. The values of the pre-factor for SIA diffusion, D_{i0}, that amounts to 2.0×10^{-8} m^2/s (4.8×10^{-8} m^2/s), and migration energy of the SIA, E_{mi}, that amounts to 0.25 eV (0.24 eV) for Fe-9at.%Cr (Fe-12.5at.%Cr) are taken according to the data [11] of SIA diffusivity dependence on the Cr content in Fe-Cr alloys.

30.3.2 CR Precipitates System

The number density of the Cr precipitates, C_n, is determined from the master equation (30.1):

$$\frac{\mathrm{d}C_n}{\mathrm{d}t} = \beta_n \left(\left(\frac{n-1}{n} \right)^{1/3} C_{n-1} - \left(1 + \left(\frac{n-1}{n} \right)^{1/3} w_n \right) \cdot C_n + w_{n+1} \cdot C_{n+1} \right). \tag{30.1}$$

Here, n is the size of the Cr precipitate, $2 \leq n \leq N_{\max}$, and C_n is set to zero for $n > N_{\max}$, as is the case for all C_n at t = 0. β_n is the absorption rate of an n-atomic cluster as obtained to account for the resulting overlapping diffusion field effects [13]:

$$\beta_n = 4\pi \sqrt[3]{\frac{3\Omega_{Cr}}{4\pi}} D_{Cr}^{irr} \frac{C_{1\mathrm{Cr}}}{\Omega_{Fe}} n^{1/3} \frac{1 + kr^{ext}}{1 + k(r^{ext} - r)}, \quad r \leq r^{\mathrm{ext}}, \tag{30.2a}$$

$$\beta_n = 4\pi \sqrt[3]{\frac{3\Omega_{Cr}}{4\pi}} D_{Cr}^{irr} \frac{C_{1\mathrm{Cr}}}{\Omega_{Fe}} n^{1/3} (1 + kr^{ext}), \quad \mathrm{r} \geq r^{\mathrm{ext}}, \tag{30.2b}$$

where Ω_{Fe} and Ω_{Cr} are the atomic volumes of bcc iron and bcc chromium; $C_{1\mathrm{Cr}}$ is the concentration of the remaining solute chromium atoms in the matrix; r^{ext} is the mean one half distance between Cr precipitate that has been taken about 1 nm according to the analysis of interference factor $S(Q)$ [7]; k is the rate at which Cr monomers are absorbed.

The chromium concentration $C_{1\mathrm{Cr}}$ is determined via:

$$C_{1\mathrm{Cr}} = C_{0\mathrm{Cr}} - \sum_{n=2}^{N_{\max}} nC_n, \tag{30.3}$$

with $C_{0\mathrm{Cr}}$ being the initial concentration of the chromium atoms.

$D_{\mathrm{Cr}}^{\mathrm{irr}}$ is the irradiation enhanced diffusion coefficient of chromium in iron according to:

$$D_{\mathrm{Cr}}^{\mathrm{irr}} = D_{\mathrm{Cr}}^{\mathrm{th}} \frac{C_{1\mathrm{v}}^{\mathrm{irr}}}{C_{1\mathrm{v}}^{\mathrm{eq}}}, \tag{30.4}$$

where $D_{\mathrm{Cr}}^{\mathrm{th}}$ is the thermal diffusion coefficient of chromium in iron, calculated according to the Arrhenius law with the experimental parameters $D_0 = 1.29 \times 10^{-4}$ m^2/s and $E_m = 2.39$ eV for Fe-12%Cr alloy [21]. $C_{1\mathrm{v}}^{\mathrm{eq}}$ and $C_{1\mathrm{v}}^{\mathrm{irr}}$ are the vacancy concentrations for the non-irradiated and irradiated state of the material, respectively, with $C_{1\mathrm{v}}^{\mathrm{eq}}$ being evaluated as in [19].

We focus on the vacancy exchange mechanism for the chromium mobility in the Fe-Cr system, which is the dominant mechanism in the Fe-12.5%Cr alloy investigated here.

The emission parameter, w_n, is calculated, taking into account the contribution of matrix frustration to the free energy of cluster distributions in binary alloys [14, 15]. This effect is typical for concentrated alloys, when the Frenkel's model of ideal cluster gas [5] is not valid and it is necessary to consider the interaction between the clusters [15] by means of the so-called exclusion volume, $V_{\mathrm{k,n}}$, i.e. the number of forbidden atomic sites (or volume normalized by the atomic volume) to a k-mer by an n-mer. In our paper it is suggested to take into account the frustration effect empirically by the use of the thermodynamic free energy expression from CALPHAD [16] with the correction suggested by Bonny et al. [17].

The emission parameter, w_n, is finally calculated by Eq. 30.5:

$$w_n = \exp\left(-\frac{\Delta\mu}{k_B T}\right) \exp\frac{4\pi\gamma^{\mathrm{cl,m}}\left(R_n^2 - R_{n-1}^2\right)}{k_B T}, \tag{30.5}$$

where $\gamma^{\mathrm{cl,m}}$ is the specific surface tension of the interface between the Cr cluster (cl) and the matrix (m); R_n is the radius of a Cr cluster of size n; k_B is the Boltzmann constant, and $\Delta\mu$ is determined via

$$\Delta\mu = \left(\mu_{\mathrm{Cr}}^{\mathrm{m}}(C_{1\mathrm{Cr}}) - \mu_{\mathrm{Cr}}^{\mathrm{cl}}\right) \cdot x_{\mathrm{Cr}}^{\mathrm{cl}} + \left(\mu_{\mathrm{Fe}}^{\mathrm{m}}(C_{1\mathrm{Cr}}) - \mu_{\mathrm{Fe}}^{\mathrm{cl}}\right) \cdot x_{\mathrm{Fe}}^{\mathrm{cl}}. \tag{30.6}$$

Here $\mu_{\mathrm{Cr}}^{\mathrm{cl}}\left(\mu_{\mathrm{Cr}}^{\mathrm{m}}\right)$ and $\mu_{\mathrm{Fe}}^{\mathrm{cl}}\left(\mu_{\mathrm{Fe}}^{\mathrm{m}}\right)$ are the chemical potentials of chromium and iron, respectively, in the precipitate cluster (matrix), and $x_{\mathrm{Cr(Fe)}}^{\mathrm{cl}}$ is the mole fraction of chromium (iron) in the Cr precipitate, which is set to 0.95 ± 0.05 according to the assumption of the equality of precipitate and matrix composition at the binodal miscibility curve. The chemical potential of chromium (iron) in both subsystems, matrix and precipitate, is taken from Eq. 30.7:

$$\mu_{\mathrm{Cr(Fe)}} = \frac{\partial}{\partial n_{\mathrm{Cr(Fe)}}}\left((n_{Cr} + n_{Fe})\frac{G}{N_\mathrm{A}}\right), \tag{30.7}$$

where $n_{Cr}(n_{Fe})$ is the number of chromium (iron) atoms in the respective Fe-Cr subsystem; N_A is the Avogadro number, and G is the total *molar* Gibbs free energy as obtained from the expression used by CALPHAD [16]:

$$G = x_{\mathrm{Cr}}G_{\mathrm{Cr}}^{\mathrm{bcc}} + x_{\mathrm{Fe}}G_{\mathrm{Fe}}^{\mathrm{bcc}} + k_B N_A T(x_{\mathrm{Cr}}\ln x_{\mathrm{Cr}} + x_{\mathrm{Fe}}\ln x_{\mathrm{Fe}}) + G_{\mathrm{ex}}^{\mathrm{bcc}} + G_{\mathrm{M}}^{\mathrm{bcc}}. \tag{30.8}$$

Here $x_{\mathrm{Cr}}(x_{Fe})$ is the chromium (iron) mole fraction – or equivalently, the concentration measured in atoms per site – in the respective Fe-Cr subsystem. $G_{\mathrm{Cr}}^{\mathrm{bcc}} \times (G_{\mathrm{Fe}}^{\mathrm{bcc}})$ is the molar free energy of pure bcc Cr(Fe) as reported [22], and $G_{\mathrm{M}}^{\mathrm{bcc}}$ is the magnetic contribution to the molar excess free energy [23], $G_{\mathrm{ex}}^{\mathrm{bcc}}$ is non-magnetic molar excess free energy according to the regular solution model [16] for the Fe-Cr system. This expression has been modified by G. Bonny [17] in order to account for the recently proposed modification of the Fe-rich phase boundary [24] for the temperature well below 800 K. We have found that the Redlich-Kister polynomial [17] could equally well be written in the following factorized form:

$$G_{\mathrm{ex}}^{\mathrm{bcc}} = x_{\mathrm{Cr}}(1 - x_{\mathrm{Cr}}) \cdot \left[20500 - 9.68 \cdot T + L(x_{\mathrm{Cr}}) \cdot \left(1 - \frac{T}{1100}\right)^3 \theta\left(1 - \frac{T}{1100}\right)\right] \text{J/mol}, \tag{30.9}$$

where

$$L(x_{\mathrm{Cr}}) = 8615.407399 + 431.3047159(2x_{\mathrm{Cr}} - 1) - 31452.7845(2x_{\mathrm{Cr}} - 1)^2 + 48134.04065(2x_{\mathrm{Cr}} - 1)^3 - 23569.11288(2x_{\mathrm{Cr}} - 1)^4 - 5625.73983(2x_{\mathrm{Cr}} - 1)^5 \quad (30.10)$$

and $\theta(x)$ is the Heavyside function being one for $x \geq 0$ and zero else. All coefficients in Eqs. 30.9 and 30.10 are given in SI units (i.e., in J/mol and K).

Again the library solver LSODA has been used to integrate the master equations (30.1, 30.2a, 30.2b, 30.3, 30.4, 30.5, 30.6, 30.7, 30.8, 30.9, and 30.10) in order to find the precipitate cluster concentrations C_n for all n up to $N_{\max} = 9000$.

30.4 Cluster Dynamics Modeling

The results from the CD modelling for the dose dependence of the free vacancy and SIA concentrations, C_{1v}^{irr} and C_{1i}^{irr}, the mean radius of the VC and mean diameter of the SIAC, $(R_{\mathrm{v}})_{\mathrm{mean}}$ and $(2R_{\mathrm{i}})_{\mathrm{mean}}$, the total number density of SIAC, N_{i}, the volume fraction of the Cr precipitates, $C_{\mathrm{v,Cr}}$, and the mean radius of the Cr precipitates, $(R_{\mathrm{Cr}})_{\mathrm{mean}}$, for Fe-12.5at.%Cr alloy are shown in the Figs. 30.1, 30.2, 30.3, and 30.4. A saturation behavior under neutron irradiation is observed for both, C_{1i} and N_{i}, at doses higher than about 0.006 dpa (Fig. 30.1).

The loop diameters $(2R_{\mathrm{i}})_{\mathrm{mean}}$ found in the simulations increase slowly with neutron irradiation and reach 5.74 and 6.25 nm for the neutron doses of 0.6 and

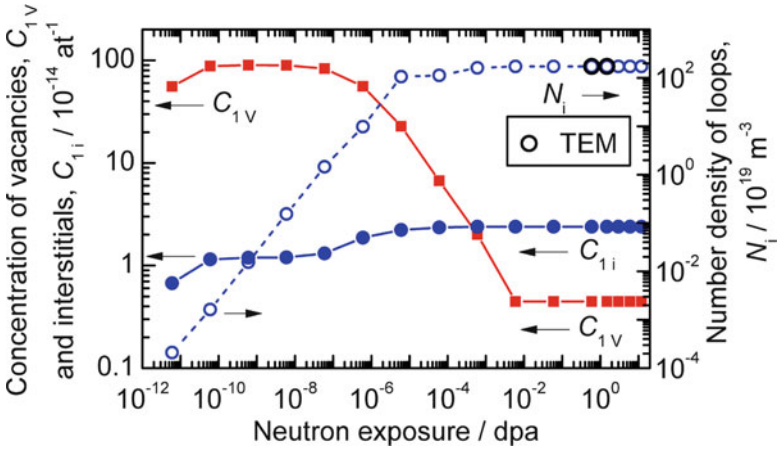

Fig. 30.1 Dose dependence of the free vacancy (SIA) concentrations, C_{1v}^{irr} (C_{1i}^{irr}), and the total number density of SIAC, Ni, for the irradiated Fe-12.5at.%Cr alloy according to the TEM experiment [2] and the CD simulations

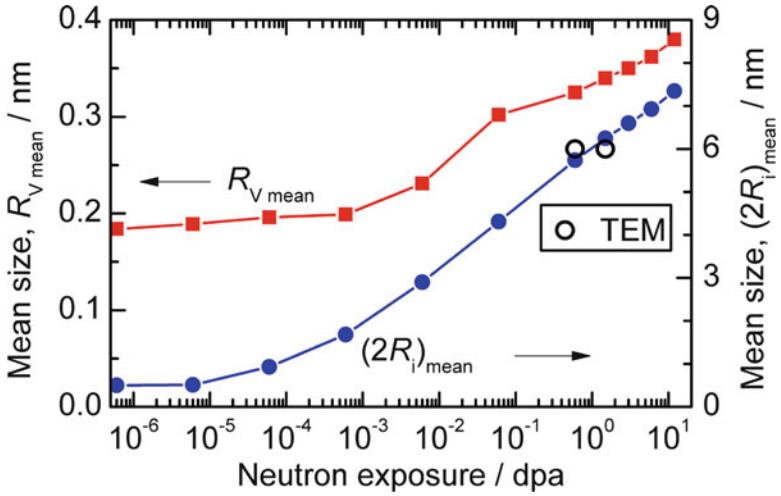

Fig. 30.2 Dose dependence of the mean radius of the VC and the mean diameter of the SIAC, (Rv)mean and (2Ri)mean, for the irradiated Fe-12.5 at.%Cr alloy according to the TEM experiment [2] and the CD simulations

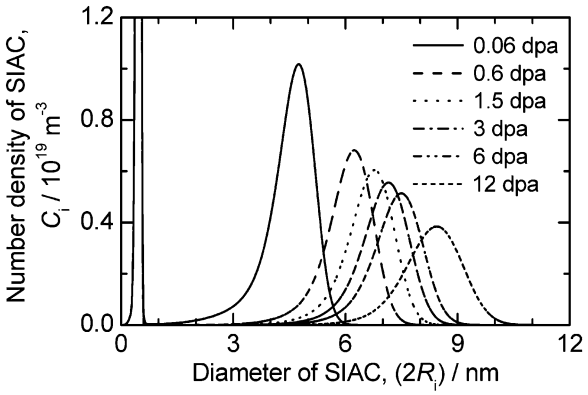

Fig. 30.3 Size distributions of self interstitial atom cluster in Fe-12.5%Cr for different irradiation conditions as obtained from the CD simulations

1.5 dpa, respectively Fig. 30.2, instead of about 6 nm for both doses as observed experimentally [1]. A value of about 1.73×10^{21} m^{-3} is found in the CD simulation for the number density of the SIAC at the experimental neutron doses of 0.6 and 1.5 dpa. The same value was observed by TEM [1].

The strong peak in the SIAC distribution at diameters of about 0.5 nm (see Fig. 30.3) is observed for all neutron exposures.

The value of $(R_v)_{mean}$ increases quite slowly up to an irradiation dose of about 6×10^{-4} dpa. Then it increases faster but does never exceed 0.5 nm (Fig. 30.2),

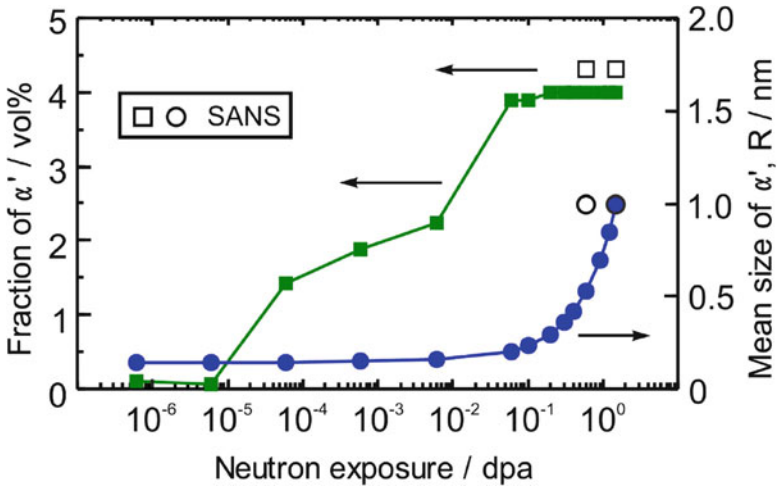

Fig. 30.4 Dose dependence of the volume fraction and mean radius of the Cr precipitates, Cv,Cr and (R_{Cr}) mean, for the irradiated Fe-12.5%Cr alloy according to the TEM experiment [2] and the CD simulations

which is the experimental resolution limit for both SANS and TEM techniques. Thus, our finding is in line with the fact, that no VC has been detected in the experimental studies [1, 2].

The Cr precipitates evolution has been found as rather sensitive to the specific surface tension $\gamma^{cl,m}$ of the interface between the precipitate cluster and the α matrix as well as to the rate k at which Cr monomers are absorbed. The values for $\gamma^{cl,m}$ of about 0.17 J/m^2 and k of about 7.94 m^{-1} are necessary to approximate reproduction of the SANS data [2] for the dose dependence of the volume fraction $C_{v,Cr}$ and the mean radius $(R_{Cr})_{mean}$ of the Cr-rich α′ precipitates by the CD simulations (Fig. 30.4). The saturation of the simulated $C_{v,Cr}$ values at about 4.0 vol% as well as the saturation of the $N_{i.}$ values are observed for the same neutron exposes.

It has been found that CD modeling according [19] to the taken into account chromium effect on the SIA diffusivity [11] provides the reproduction of experimental TEM data [1] on N_i and $(2R_i)_{mean}$ very roughly for Fe-9at.%Cr alloy.

30.5 Discussion

In accordance with the compared kinetic Monte Carlo simulations and CD [25], the deviation of the cluster system from the ideal gas cluster model [5] must be taken into account in CD scheme, when the solute concentration exceeds the order of 1%

atomic in AlZr alloys. Because of the complexity of calculations [25], the subject of interest is to estimate a-priori the frustration effect in the binary alloys. It has been revealed [26] that the applicability of the concept of the uniform supersaturation ignoring the exclusion volume in the cluster system depends not on the absolute value of solute concentration but on the value of dimensionless parameter a and is defined as:

$$a = \frac{C_0 - C_{eq}}{C_{cl}}, \tag{30.11}$$

where C_0, C_{eq} and C_{cl} are the initial concentration, solubility limit and concentration of solute atoms in the cluster (precipitate), respectively.

The small value of parameter a ($a << 1$) corresponds to the thin layer of the depletion zone surrounding a cluster, i.e. a small value of exclusion volume. This parameter is about 0.002 for Fe-9at.%Cr alloy. Hence, it can be expected that no frustration effect for Fe-9at.%Cr alloy is observed and it is possible to consider this alloy as dilute Fe-Cr alloy. This statement is confirmed by the absence of the interference effect in SANS study [3]. Parameter a is about 0.039 for Fe-12.5a% Cr alloy, for which the interference effect is observed by SANS. Hence, this alloy has been considered as the concentrated Fe-Cr alloy. On the other hand, the values of parameter a as well as of the upper limits of constant exclusion volume estimated from SANS [7] are not so high for irradiated Fe-12.5a%Cr alloy. That is why taking into account the frustration effect empirically by the use of the thermodynamic free energy expression [17] is found successful in CD modeling of Cr precipitates in this alloy. The complimentary consideration of the diffusion field effects [13] provides the best fit to SANS data for value of the specific surface tension $\gamma^{\mathrm{cl,m}}$ of about 0.17 J/m^2 (instead of 0.028 J/m^2 in [7], where these effects are ignored). It should be emphasized that the obtained result is in a good agreement with the data of $\gamma^{\mathrm{cl,m}}$ obtained [27] by the Cluster Expansion method: 0.218, 0.155, and 0.048 J/m^2 for the coherent interfaces [100], [111] and [110], respectively.

The unsuccessful application of the CD scheme in our study to the irradiated Fe-9at.%Cr alloy, which includes the dislocation loops decorated by Cr atoms, shows the necessity to consider the formation and migration of Fe-Cr interstitial as an additional link between the CD master equations for the self-defects and the CD master equations for the Cr precipitates in this alloy.

The assumption of the constant composition of Fe-Cr clusters under neutron irradiation needs further examination too. In fact, $x^{\mathrm{cl}}_{\mathrm{Cr(Fe)}}$ changes under neutron irradiation from the thermal equilibrium value of about 0.085 for T = 573 K to its value of about 0.95 $\pm$ 0.05 for the expose with the dose less than 0.6 dpa. Hence, the population of Fe-Cr clusters has been described by the distribution function not only on size but also on composition, $f(C_{Cr\_cl}, n)$, or two-component distribution function, $f(n_{\mathrm{Cr}}, n)$, on the number of chromium atoms in cluster (n_{Cr}) and the total

number of atoms in cluster (n). The corresponding master equation is presented by formulas (30.12–30.15):

$$\frac{\partial f(n_{Cr}, n)}{\partial t} = -\left(\beta_{1,2}(n_{Cr}, n) + \alpha_{1,2}(n_{Cr}, n)\right) \cdot f(n_{Cr}, n) + \alpha(n_{Cr}+1, n+1) \cdot f(n_{Cr}+1, n+1) + \alpha(n_{Cr}, n+1) \cdot f(n_{Cr}, n+1) + \beta(n_{Cr}-1, n-1) \cdot f(n_{Cr}-1, n-1) + \beta(n_{Cr}, n-1) \cdot f(n_{Cr}, n-1) \quad (30.12)$$

Here $\beta(n_{Cr}-1, n-1)$ and $\beta(n_{Cr}, n-1)$ describe the attachment of one atom of chromium and one iron atom, respectively, by the cluster containing n_{Cr} chromium atoms and (n−n_{Cr}) iron atoms; $\beta_{1,2}(n_{Cr}, n)$ and $\alpha_{1,2}(n_{Cr}, n)$are determined following the probabilistic interpretation of the attachment and emission coefficients. In the case of a single component system $\Delta t \cdot \beta[(n) \Rightarrow (n+1)]$ there is a probability in the time interval Δt that a single monomer is added to the cluster of size (n). In the case of a two-component system $\Delta t \cdot \beta(n_{Cr}, n)$ there is a probability in the time interval Δt that any single monomer of the first or second component is added to the cluster (n_{Cr}, n) excluding the event when both monomers are added simultaneously to this cluster.

$$\beta_{1,2} = \beta_1(n_{Cr}, n) + \beta_2(n_{Cr}+1, n) - 2\beta_1(n_{Cr}, n)\beta_2(n_{Cr}+1, n)\Delta t. \quad (30.13)$$

Here Δt can be estimated by the Eq. 30.14:

$$\Delta t = \frac{b^2}{D^k_{1,2}}, \quad (30.14)$$

where b is the thickness of the boundary between a cluster and a matrix and $D^k_{Fe} \approx D^k_{Cr} = D^k_{1,2}$. The latter is supported by the experimental ratio between the diffusivity of iron and chromium in the iron matrix for the diffusion limited regime [21].

Coefficients $\alpha_{1,2}(n_{Cr}, n)$are determined in the same way from Eq. 30.15:

$$\alpha_{1,2}(n_{Cr}, n) = \alpha_1(n_{Cr}, n) + \alpha_2(n_{Cr}+1, n) - 2\alpha_1(n_{Cr}, n)\alpha_2(n_{Cr}+1, n)\Delta t. \quad (30.15)$$

Here, the emission coefficients $\alpha_1(n_{Cr}, n)$and $\alpha_2(n_{Cr}+1.n)$ are determined from the coefficients $\beta_1(n_{Cr}, n)$ and $\beta_2(n_{Cr}+1, n)$ according to the detailed balance principle.

The size dependence of n_{Cr}/n on the size of Fe-Cr precipitates in Fe-1.5at.%Cr alloy calculated according to the master equations (30.12, 30.13, 30.14, and 30.15) for the irradiation times of 6×10^{-9} and 6×10^{-4} is presented in Fig. 30.5. A difference in the composition of Fe-Cr precipitates with the size less than 30 monomers has been found for these times. The following study of the considered effect needs a significant increase in computer calculations.

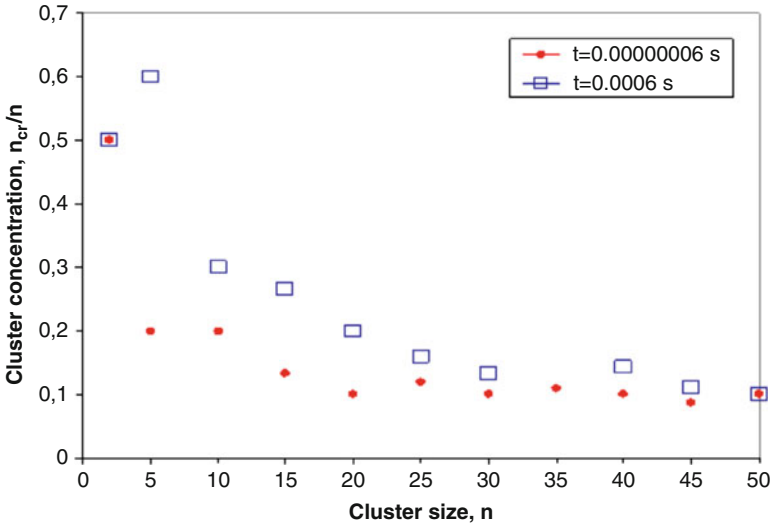

Fig. 30.5 The size dependence of n_{Cr}/n on size of Fe-Cr precipitates in Fe-1.5at.%Cr alloy calculated according to master equations (30.12, 30.13, 30.14, and 30.15) for the different irradiation times

30.6 Conclusion

Cluster dynamic (CD) simulations [19], including the effect of the chromium concentration on the SIA diffusivity [11], are able to reproduce the experimental TEM data [1] for Fe-12.5at.%Cr on the SIAC size distribution. The saturation behavior of the total number density of SIAC in neutron irradiated Fe-12.5at.%Cr model alloys for the neutron expose greater than 0.006 dpa has been predicted. The CD simulations also indicate the presence of VC with radii less than 0.5 nm and a strong SIAC peak with a mean diameter of about 0.5 nm, both invisible in SANS and TEM experiments because of the resolution limits of these techniques. The ratio of the exceeding solute concentration to the concentration of solute atoms in a cluster (precipitate) as well as SANS study can be used to estimate a-priory the effect of the exclusion volume in CD simulations of Cr precipitates in Fe-Cr alloys.

Taking into account the frustration effect empirically by the use of the thermodynamic free energy expression [17] is sufficient for CD modeling of Cr precipitates in the irradiated Fe-12.5at.%Cr alloy. By adjusting the specific surface tension between the α matrix and the α' precipitates and the rate at which Cr monomers are absorbed, it is possible to reproduce the SANS data [2] for this alloy. The resulting specific interface energy of 0.17 J/m^2 is in a good agreement with calculations according to the Cluster Expansion method [27]. Taking into account the formation and migration of Fe-Cr interstitial as an additional link between the CD master equations for self-defects and the CD master equations for Cr precipitates, can

improve CD results for irradiated Fe-9at.%Cr alloy. The change of the composition of Fe-Cr precipitates due to irradiation has to be taken into account in the following CD modeling.

Acknowledgment This work was supported by the European Commission within the Collaborative Project GETMAT.

References

1. Matijasevic M, Almazouzi A (2008) Effect of Cr on the mechanical properties and microstructure of Fe-Cr model alloys after n-irradiation. J Nucl Mat 377:147
2. Bergner F, Ulbricht A, Heintze C (2009) Estimation of solubility limit of Cr in Fe at 300°C from small-angle scattering in neutron irradiated Fe-Cr alloys. Scripta Materialia 61:1060
3. Ulbricht A, Heintze C, Bergner F, Eckerlebe H (2010) SANS investigation of a neutron irradiated Fe-9 at % Cr alloy. J Nucl Mat 407:29
4. Heintze C, Bergner F, Ulbricht A, Eckerlebe H (2011) The microstructure of neutron-irradiated Fe-Cr alloys: a small angle scattering study. J Nucl Mat 409:106
5. Frenkel J (1955) Kinetic theory of liquids. Dover Publications, New York, pp 1–483
6. Staron P (1997) PhD thesis, Universität Hamburg, also published as Report GKSS 97/E/53, GKSS Forshungszentrum Geesthacht
7. Gokhman A, Ulbricht A, Birkenheuer U, Bergner F (2011) Cluster dynamics study of neutron irradiation induced defects in Fe-12.5at%Cr alloy. Solid State Phenom 172–174:449
8. Kinning DJ, Thomas Hard-sphere EL (1984) interaction between spherical domains in diblock copolymers. Macromolecules 17:1712
9. Malerba L, Caro A, Wallenius J (2008) Multiscale modeling of radiation damage and phase transformations: the challenge of Fe-Cr alloys. J Nucl Mat 382:112
10. Christien F, Barbu A (2004) Modelling of copper precipitation in iron during thermal aging and irradiation. J Nucl Mat 324:90
11. Terentyev D, Olsson P, Klaver TPC, Malerba L (2008) On the migration and trapping of single self-interstitial atoms in dilute and concentrated Fe-Cr alloys: atomistic study and comparison with resistivity recovery experiments. Comput Mat Sci 43:1183
12. Olsson P, Domain C, Wallenius J (2007) *Ab initio* study of Cr interactions with point defects in bcc Fe. Phys Rev B75:014110
13. Clouet E, Barbu A, Laé L, Martin G (2005) Precipitation kinetics of Al_3Zr and Al_3Sc in aluminum alloys modeled with cluster dynamics. Acta Mater 53:2313–2325
14. Lepinoux J (2009) Modelling precipitation in binary alloys by cluster dynamics. Acta Mater 57:1086–1094
15. Lepinoux J (2006) Contribution of matrix frustration to the free energy of cluster distributions in binary alloys. Philos Mag 86:5053
16. Andersson J-O, Sundman B (1987) Thermodynamic properties of the Cr-Fe system. CALPHAD 11:83
17. Bonny G, Terentyev D, Malerba L (2010) New contribution to the thermodynamics of Fe-Cr Alloys as Base for Ferritic Steels. JPEDAV 31:439–444. doi:10.1007/s11669-010-9782-91547-7037 (ASM International, Basic and Applied Research: Section I)
18. LSODA is part of the ODEPACK provided by Alan C. Hindmarsh on the CASC server of the Lawrence Livermore National Laboratory, Livermore, CA 94551, USA
19. Gokhman A, Bergner F (2010) Cluster dynamics simulation of point defect clusters in neutron irradiated pure iron. Radiat Eff Defects Solids 165:216
20. Hardouin Duparc A, Moingeon C, Smetaninsky-de-Grande N, Barbu A (2002) Microstructure modeling of ferritic alloys under high flux 1 MeV electron irradiations. J Nucl Mat 302:143

21. Wolfe RA, Paxton HW (1964) Diffusion in BCC metals. Trans Metall Soc AIME 230:1426
22. Dinsdale AT (1991) SGTE data for pure elements. CALPHAD 15:317
23. Hillbert M, Jarl M (1978) A model for alloying effects in ferromagnetic metals. CALPHAD 2:227
24. Bonny G, Terentyev D, Malerba L (2008) On the miscibility gap of Fe-Cr alloys. Scripta Materialia 59:1193
25. Lepinoux J (2010) Comparing kinetic Monte Carlo simulations with cluster dynamics: what can we learn about precipitation? Application to AlZr alloys. Philos Mag 90:3261
26. Kuchma AE, Kuni FM, Shchekin AK (2009) Nucleation stage with non-steady growth of supercritical gas bubbles in a strong supersaturated liquid solution and the effect of excluded volume. Phys Rev E80:061125
27. Nguyen-Manh Duc, Yu M, Lavrentiev SL, Dudarev CR (2008) The Fe-Cr system: atomistic modeling of thermodynamics and kinetics of phase transformations. Physique 9:379